International Journal of Biochemistry and Cell Biology 171 (2024) 106571

Contents lists available at ScienceDirect

International Journal of Biochemistry and Cell Biology

journal homepage: www.elsevier.com/locate/biocel

The inositol-requiring enzyme 1 (IRE1) endoplasmic reticulum stress pathway promotes MDA-MB-231 cell survival and renewal in response to the aryl-ureido fatty acid CTU

Md Khalilur Rahman [a,1], Balasubrahmanyam Umashankar [a,2], Hassan Choucair [a,3], Kirsi Bourget [a], Tristan Rawling [b], Michael Murray [a,*]

[a] Pharmacogenomics and Drug Development Group, Discipline of Pharmacology, School of Medical Sciences, and School of Pharmacy, Faculty of Medicine and Health, University of Sydney, NSW 2006, Australia
[b] School of Mathematical and Physical Sciences, Faculty of Science, University of Technology Sydney, Ultimo, NSW 2007, Australia

ARTICLE INFO

Keywords:
Pro-inflammatory mediators
NF-κB
XBP-1s
IRE1
Self-renewal
Mammosphere assay

ABSTRACT

Current treatment options for triple-negative breast cancer (TNBC) are limited to toxic drug combinations of low efficacy. We recently identified an aryl-substituted fatty acid analogue, termed CTU, that effectively killed TNBC cells in vitro and in mouse xenograft models in vivo without producing toxicity. However, there was a residual cell population that survived treatment. The present study evaluated the mechanisms that underlie survival and renewal in CTU-treated MDA-MB-231 TNBC cells. RNA-seq profiling identified several pro-inflammatory signaling pathways that were activated in treated cells. Increased expression of cyclooxygenase-2 and the cytokines IL-6, IL-8 and GM-CSF was confirmed by real-time RT-PCR, ELISA and Western blot analysis. Increased self-renewal was confirmed using the non-adherent, in vitro colony-forming mammosphere assay. Neutralizing antibodies to IL-6, IL-8 and GM-CSF, as well as cyclooxygenase-2 inhibition suppressed the self-renewal of MDA-MB-231 cells post-CTU treatment. IPA network analysis identified major NF-κB and XBP1 gene networks that were activated by CTU; chemical inhibitors of these pathways and esiRNA knock-down decreased the production of pro-inflammatory mediators. NF-κB and XBP1 signaling was in turn activated by the endoplasmic reticulum (ER)-stress sensor inositol-requiring enzyme 1 (IRE1), which mediates the unfolded protein response. Co-treatment with an inhibitor of IRE1 kinase and RNase activities, decreased phospho-NF-κB and XBP1s expression and the production of pro-inflammatory mediators. Further, IRE1 inhibition also enhanced apoptotic cell death and prevented the activation of self-renewal by CTU. Taken together, the present findings indicate that the IRE1 ER-stress pathway is activated by the anti-cancer lipid analogue CTU, which then activates secondary self-renewal in TNBC cells.

Abbreviations: ATF6, activating transcription factor 6; COX-2, cyclooxygenase-2; CTU, 16-{[4-chloro-3-(trifluoromethylphenyl]carbamoyl}amino)hexadecanoic acid; CYP, cytochrome P450; DMEM, Dulbecco's Modified Eagle's Medium; DMSO, dimethylsulfoxide; ER, endoplasmic reticulum; EsiRNA, endoribonuclease prepared siRNA; FBS, fetal bovine serum; GM-CSF, granulocyte-macrophage colony-stimulating factor; IKK, IκB kinase; IκB, inhibitor of nuclear factor kappa B; MTT, 3–4,5-Dimethylthiazol-2-yl-2,5-diphenyltetrazolium bromide; NF-κB, nuclear factor-κB; IL-6, interleukin-6; IL-8, interleukin-8; IRE1, inositol-requiring enzyme 1; PBS, phosphate-buffered saline; PERK, PKR-like ER kinase; RT-PCR, real-time polymerase chain reaction; TNBC, triple negative breast cancer; UPR, unfolded protein response; XBP1s, X box binding protein-1 spliced form.

* Correspondence to: School of Pharmacy, Faculty of Medicine and Health, University of Sydney, NSW 2006, Australia.
E-mail address: michael.murray@sydney.edu.au (M. Murray).
[1] Mucpharm Pty Ltd, Kogarah, NSW, 2217, Australia
[2] Molecular and Integrative Cystic Fibrosis Research Group, School of Biomedical Sciences, Faculty of Medicine and Health, University of New South Wales, New South Wales, 2052, Australia
[3] School of Health Sciences, Faculty of Medicine, Nursing and Midwifery and Health Sciences, The University of Notre Dame Australia, Chippendale, New South Wales, 2007, Australia

https://doi.org/10.1016/j.biocel.2024.106571
Received 22 December 2023; Received in revised form 4 April 2024; Accepted 8 April 2024
Available online 11 April 2024

1. Introduction

The treatment of patients with triple-negative breast cancer (TNBC) usually involves toxic drug combinations. There is an urgent need for new agents that are well tolerated and exhibit improved efficacy. The anti-cancer activities of ω-3 polyunsaturated fatty acids, such as eicosapentaenoic acid, could be a potential source of new agents for the treatment of TNBC (Augimeri et al., 2023; Bobin-Dubigeon et al., 2022; Chajès et al., 2012; Rose and Connolly, 2000; Wiseman et al., 2022). ω-3 Polyunsaturated fatty acids undergo biotransformation to diverse lipid mediators that modulate cell growth and homeostasis, including epoxides generated by cytochromes P450s (CYPs; Spector, 2009; Al-Bahlani et al., 2017; Woodcock et al., 2018). While CYPs have been intensively studied for their roles in xenobiotic oxidation, these enzymes also mediate the oxidation of important endobiotics such as polyunsaturated fatty acids and steroids (Zhang et al., 2013; Rendic and Guengerich, 2015; Newell et al., 2019). CYP-mediated oxidation of eicosapentaenoic acid generates the ω-3–17,18-epoxide that has been found to selectively inhibit cell proliferation and activate apoptosis, whereas the regioisomeric epoxides did not decrease cell viability (Cui et al., 2011). In addition, synthetic ω-3 monoepoxides of long-chain saturated fatty acids also impair the viability of MDA-MB-231 TNBC cells (Dyari et al., 2014). However, the susceptibility of fatty acid epoxides to hydration by soluble epoxide hydrolase rapidly terminates their actions *in vivo*, which prevents their development as drugs (Fleming et al., 2007; Inceoglu et al., 2008). Instead, stable ω-3 and ω-6 epoxide mimics have been developed by bioisosteric replacement of the unstable epoxide moieties with urea (Liu et al., 2001; Falck et al., 2009, 2014); many of these mimics retain the biological actions of the epoxides. We reported that an aryl-substituted ureido-fatty acid, termed CTU (Fig. 1A), killed TNBC cells *in vitro* and was well tolerated in mice *in vivo* (Rawling et al., 2017).

The endoplasmic reticulum (ER) regulates the correct folding of proteins and their trafficking to other cellular destinations (Xu et al., 2005; Hetz et al., 2020). When misfolded and damaged proteins accumulate in the ER the unfolded protein response (UPR) is activated, which is mediated by the ER stress sensors inositol requiring enzyme 1α/β (IRE1), PKR-like ER kinase (PERK) and activating transcription factor 6α/β (ATF6) (Xu et al., 2005; Kimata et al., 2007). The UPR halts protein translation and activates protein folding to reestablish ER homeostasis but, if the stress is prolonged, cell death is triggered (Xu et al., 2005; Kimata et al., 2007; Luo et al., 2022). Recently, CTU was found to target the tumor cell mitochondrion and uncouple electron transport. ATP production was impaired and reactive oxygen species production was increased, which activated the PERK pathway of ER stress and apoptotic cell death (Choucair et al., 2022).

Cancer cells survive cytotoxic drug exposure by activating survival signals and/or by deactivating pro-death signals (Hassan et al., 2014). Although CTU is the prototype of a new class of agents with promising anti-cancer properties, nevertheless it appeared that a proportion of TNBC cells remained viable after treatment. The present study was

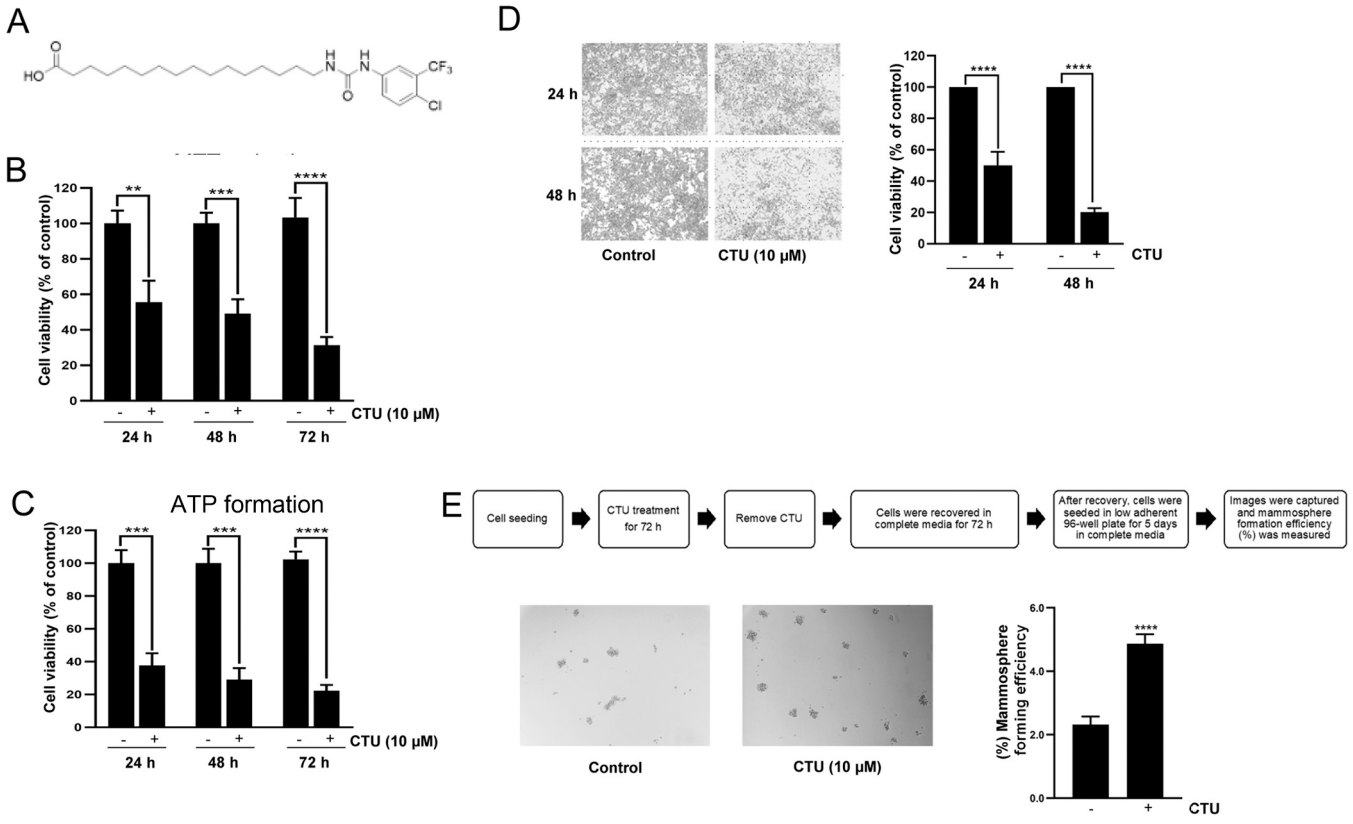

Fig. 1. Increased self-renewal capacity of residual MDA-MB-231 cells after CTU treatment. (A) Structure of CTU. (B) CTU-mediated time-dependent decreases in MTT reduction. Cells (1×10^4/well) were treated with CTU (10 μM) for 24, 48 h or 72 h. MTT was added as described in Materials and Methods and the absorbance at 540 nm was measured. (C) CTU-mediated time-dependent decreases in ATP formation. Cells (7.5×10^4/well) were treated with CTU (10 μM). ATP formation was assessed using the CellTiter-Glo® luminescent assay as described in Materials and Methods. (D) Crystal Violet staining analysis of the residual surviving cell populations after CTU treatment. Cells (1.5×10^5/well) were treated with CTU (10 μM) for 24 or 48 h, stained with 0.5 % crystal violet and images were captured as described in Materials and Methods. (E) Mammosphere formation in CTU-treated (10 μM, 72 h) MDA-MB-231 cells. Cells (1.5×10^5/well) were treated with CTU (10 μM) for 72 h. Surviving cells were incubated for a further 72 h in complete medium and then seeded (1×10^3/well) on ultra-low attachment plates. DMEM/F12 medium containing B27-supplement and EGF (20 ng/ml) was added and incubations were continued for a further 5 d. Images were captured and analyzed as described in Materials and Methods. Data are presented as mean ± standard error (SEM) of three or more independent experiments, with at least two internal replicates. Different from corresponding control: ** $p < 0.01$, *** $p < 0.001$, **** $p < 0.0001$.

conducted to evaluate the mechanisms by which residual tumor cell populations survived CTU treatment. The principal finding to emerge was that the self-renewal capacity of residual cell populations was attributable to the production of major pro-inflammatory mediators, including IL-6, IL-8, GM-CSF and cyclooxygenase-2 (COX-2). CTU promoted the formation of these mediators by activating the IRE1 arm of ER-stress that in turn activated NF-κB and XBP-1 signaling.

2. Materials and methods

2.1. Biochemicals and reagents for cell culture

Unless otherwise stated biochemicals were obtained from Sigma Aldrich (Castle Hill, NSW, Australia). The primary antibodies anti-IRE1 (3294 S), anti-XBP1s (12782 S), anti-phospho-NF-κB p65 (3031), anti-NF-κB p65 (8242), anti-phospho-inhibitor of NF-κB (IκB; 2859), anti-IκB (4812) and anti-XBP1s (12782) were from Cell Signaling Technology (Arundel, QLD, Australia). Anti-β-actin (C47778) and anti-COX-2 (sc-19999) primary antibodies were obtained from Santa Cruz Biotechnology (Dallas, TX). Anti-phospho-IκB kinase (IKK) α/β (ab178870) was from Abcam (Melbourne, VIC, Australia) and anti-phospho-IRE1 (NB100–2323) was from Novus Biological (Noble Park, VIC, Australia). Alexa fluor-conjugated anti-mouse (4408 S), anti-rabbit (4412 S) IgG, the Dylight-conjugated goat anti-mouse (5470 S) and goat anti-rabbit (5151 S) secondary antibodies were purchased from Cell Signaling Technology. The neutralizing antibodies against IL-6 (RDSMAB206SP), IL-8 (RDSMAB208SP), GM-CSF (RDSMAB215SP), CXCL1 (RDSMAB275) and IgG1 (RDSMAD9894) were purchased from R&D Systems (Noble Park, VIC, Australia).

Endoribonuclease prepared siRNA (esiRNA) directed against human IRE1 (EHU002721), XBP1 (EHU069131), NF-κB (EHU069421) and GAPDH (EHU146741) were obtained from Sigma Aldrich. X-treme GENE transfection reagent siRNA was from Roche (Grenzach-Wyhlen, Germany).

CTU was synthesized as described previously (Rawling et al., 2017). Chemical inhibitors and other research chemicals were obtained from Sigma Aldrich or Cayman Chemicals (Ann Arbor, MI). General analytical grade laboratory chemicals and HPLC grade solvents were obtained from LabScan (Lomb Scientific, Taren Point, NSW, Australia) or Ajax Chemicals (Sydney, NSW, Australia).

Low glucose Dulbecco's Modified Eagle's Medium (DMEM) and RPMI medium were from Sigma Aldrich. L-Glutamine was from Life Technologies (ThermoFisher Scientific, North Ryde, NSW, Australia), fetal bovine serum (FBS), phosphate-buffered saline (PBS), penicillin and streptomycin and trypsin/EDTA were from Sigma Aldrich.

2.2. Cell culture

The human MDA-MB-231, HCC1806 and SKBR3 breast cancer cell lines and the HeLa cervical carcinoma cell line were obtained from ATCC (American Type Culture Collection, Manassas, VA, USA). MDA-MB-231 and HeLa cells were cultured in DMEM-low glucose medium, while HCC1806 and SKBR3 cells were cultured in RPMI-1640 medium supplemented with 10 % FBS and 1 % penicillin/streptomycin. Cells were grown in a humidified incubator in a 5 % CO_2 atmosphere at 37 °C. Cells at 80–90 % confluence were harvested using trypsin/EDTA after washing in PBS. Trypsin was neutralized by adding DMEM medium containing 10 % FBS and removed by centrifugation (290 x g; 5 min). The cell pellet was resuspended in DMEM and cells were stained with 0.4 % trypan blue and counted (Countess; Invitrogen, Mount Waverley, VIC, Australia).

2.3. Microscopy

Crystal violet staining and light microscopy were used to evaluate CTU cytotoxicity. MDA-MB-231 cells were plated at a density of 1.5 × 10^5/well in 6-well plates and incubated overnight at 37 °C. After serum removal cells were treated with CTU for 24 or 48 h. Following treatment, cells were stained with 0.5 % crystal violet and then washed in water three times to remove residual stain. Cell images were captured using a CKX41 inverted microscope (40x magnification) equipped with an Altra 20 camera (Olympus, Notting Hill, VIC, Australia) and subjected to analysis with GetIT software (Soft Imaging System, Germany) software.

2.4. Cell viability and apoptosis

Cell viability was assessed using the MTT reduction assay. MDA-MB-231 cells were seeded into 96-well plates (1 × 10^4/well) and, after 24 h, serum was removed, and culture was continued for a further 24 h. Cells were then treated with CTU (1, 10 or 40 μM) in dimethylsulfoxide (DMSO; final concentration 0.1 %) for 24 or 48 h; control cells received serum-free DMEM alone. At the end of the treatments, 25 μL of MTT solution (2.5 mg/ml) was added to each well (37 °C; 5 % CO_2). After 2 h the supernatant was removed, the product was dissolved in 100 μL DMSO and the absorbance was measured at 540 nm in a Victor 3 V 1420 multi-label spectrophotometer (Perkelmer, Glen Waverley, VIC, Australia).

ATP formation was assessed using the CellTiter-Glo® luminescent assay (Promega; Annandale, NSW, Australia) as described previously (Dyari et al., 2014). Confluent MDA-MB-231 cells (80–90 %) were harvested using Trypsin/EDTA, washed in PBS and then seeded in 24-well plates (7.5 × 10^4/well). Cells were then treated with various concentrations of CTU (1, 10 or 40 μM) in DMSO (final concentration 0.1 %) for 24 or 48 h; control cells received serum-free DMEM alone. Luminescence was measured in a Victor 3 V 1420 multi-label counter.

The activation of CTU-mediated apoptosis was measured using Caspase-Glo 3/7 assays (Promega, Alexandria, NSW, Australia) as described previously (Dyari et al., 2014). MDA-MB-231 cells were plated in black-walled 96 well plates at a density of 7 × 10^3/well and allowed to adhere overnight. Twenty-four h after serum removal, cells were treated with CTU (10 μM; 24 h) and luminescence was measured in a Victor 3 V 1420 multi-label counter.

2.5. Mammosphere formation assay

Human MDA-MB-231 cells were plated at a density of 1.5 × 10^5/well, incubated overnight and then serum was removed. After 24 h cells were treated with CTU (10 μM) for 72 h. The CTU-containing medium was removed and surviving cells were incubated for a further 72 h in complete medium containing neutralizing antibodies against IL-8 (500 ng/ml), IL-6 (500 ng/ml) or GM-CSF (10 μg/ml); antibodies did not alter control cell viability. In other experiments, surviving cells were incubated for a further 72 h in complete medium containing chemical inhibitors of COX-2 (CAY 10404; 0.1 μM), IκB-kinase (BAY 11–7082; 5 μM), XBP1 (toyocamycin; 0.1 μM) or IRE1α (GSK2850163; 10 μM).

After these treatments, cells were trypsinised and seeded (1 × 10^3/well) on ultra-low attachment surface plates (Corning, Silverwater, NSW, Australia). DMEM/F12 medium containing B27-supplement and EGF (20 ng/ml) was added and incubations were continued for a further 5 d. During this period cells were incubated in medium that did not contain inhibitors or neutralizing antibodies. Images were captured using a light microscope and digital camera and mammosphere formation efficiency (%) was determined: (number of mammospheres > 40 μm/number of cells seeded) × 100.

2.6. mRNA extraction and real time polymerase chain reaction (RT-PCR)

Human MDA-MB-231 cells were seeded on 6-well plates (1.5 × 10^5 cells per well) and incubated for 24 h in serum-free medium. Cells were then treated with CTU (10 μM) or DMSO (control) for 24 h. RNA was extracted (ISOLATE II RNA Mini Kit, Meridian Bioscience, Cincinnati,

OH) and quantified (NanoDrop; Thermo Fisher Scientific, Macquarie Park, NSW, Australia). In RT-PCR reactions, master-mixes were prepared for each gene of interest, comprising SYBR green mix, reverse transcriptase (Applied Biosystems, Scoresby, VIC, Australia) and appropriate primers (Sigma; Table S1) in a final volume of 20 μl. Amplification conditions were optimized for each gene, and gene expression was quantified using a Rotor-Gene 6000 thermal cycler (Corbett Life Science, Sydney, NSW, Australia). Relative mRNA expression was calculated using the ΔΔCT method with β-actin as housekeeping gene.

2.7. mRNA library preparation, RNA-seq and sequencing analysis

RNA from CTU-treated MDA-MB-231 cells (10 μM, 24 h) was subjected to RNA-seq analysis, sequencing and bioinformatics analysis by the Australian Genome Research Facility (Parkville, VIC, Australia). RNA libraries were prepared using an Illumina Truseq Stranded Total RNA kit (San Diego, USA). Briefly, ribosomal ribonucleic acid (rRNA) was removed from RNA samples using biotinylated, target-specific oligos combined with Ribo-Zero rRNA removal beads. Purified RNA was fragmented and then converted into the first-strand cDNA using SuperScript II Reverse Transcriptase (Invitrogen) and random primers. To achieve high strand specificity, dTTP was replaced with dUTP in the Second Strand Marking Mix and second-strand cDNA was synthesized using DNA Polymerase I and RNase H. In the adaptor ligation step, 3′ ends of blunt fragments were adenylated by adding a single 'A' nucleotide. The addition of 'T' nucleotides at the 3′ end helped ligate the adaptor to the fragment. The product was amplified via PCR (13 cycles) and purified to create the final cDNA library.

Primary sequence data were generated using the Illumina bcl2fastq 2.18.0.12 pipeline. Sequence files were generated in a standard FASTQ format and sequence reads were aligned against the *Homo sapiens* genome (Build version HG38). The Tophat aligner (v2.0.14) was used to map reads to genomic sequences, and alignment files were rendered in the compressed BAM format. The counts of reads mapping to genes were summarized using the human annotation (Genecode v25) as reference. The EdgeR package was used to perform differential expression analysis and the GLM model was used to compare differential expression between the groups. To rank genes that were differentially expressed above a specified threshold, the glmTreat function was used. IPA software was used in bioinformatics analysis to identify potential pathways involving the differentially expressed genes. Data were uploaded to the Gene Expression Omnibus repository (accession number GSE166312: Next Generation Sequencing Facilitates Quantitative Analysis of CTU-treated Human breast MDA-MB-231 cells Transcriptomes).

2.8. Electrophoresis and immunoblotting

Cells at 80–90 % confluence were harvested with trypsin/EDTA and washed with cold PBS before addition of lysis buffer (10 mM Tris buffer, pH 6.8) supplemented with 150 mM NaCl, 0.5 % SDS, 1 % Triton X-100, 0.04 mM EDTA and protease/phosphatase inhibitor cocktail (Cell Signaling Technology). Cellular protein was electrophoresed on 7.5–12 % SDS polyacrylamide gels as outlined previously, transferred to nitrocellulose membranes (0.2 μm) and subjected to Western immunoblotting essentially as described previously (Murray, 1992). Immunoreactive proteins were identified using IRDye conjugated goat anti-mouse or goat anti-rabbit IgG as secondary antibody (Li-Cor Biosciences, Lincoln, NE) and analyzed on an Odyssey Infrared Imaging System with Image Studio Light software (Li-Cor Biosciences).

2.9. ELISA

The concentrations of pro-inflammatory cytokines and PGE_2 in cell culture medium were quantified by ELISA: IL-6, IL-8, GM-CSF kits (R&D Systems) and PGE_2-Monoclonal ELISA kit (Cayman). Cells were seeded (1.5×10^5/well) in complete medium, allowed to adhere overnight (5 % CO_2 at 37 °C), and serum was removed. Twenty-four h after treatment medium was collected and centrifuged, and ELISA assays were performed.

2.10. Transfection of esiRNA

MDA-MB-231 cells were seeded in 6 well plates (7.5×10^4/well) in DMEM medium supplemented with 10 % serum (without antibiotics) and incubated overnight at 37 °C. A mixture of X-tremeGENE siRNA transfection reagent (0.25 %), 2 μg esiRNA, and Opti-MEM I was incubated at room temperature for 20 min to form a transfection complex, and then the mixture was added to cells (40–50 % confluence) in Opti-MEM I containing 10 % serum. 'Scrambled' eGFP esiRNA was used as the negative control. After 48 h, the transfection medium was replaced with serum-free Opti-MEM I, and cells were incubated for another 24 h, after which they were treated with CTU for 24 h, harvested and analyzed.

2.11. Statistics

Data are presented as mean ± standard error (SEM) of three or more independent experiments, with at least two internal replicates. Data from multiple treatments were analyzed by analysis of variance and PLSD testing and differences between control and treatment groups were identified using the Student's t-test (Statview, Abacus Corp, Berkley, CA).

3. Results

3.1. Self-renewal of MDA-MB-231 cell populations after CTU treatment

Consistent with previous observations, CTU decreased the viability of MDA-MB-231 TNBC cells (Dyari et al., 2014). Thus, CTU (10 μM) decreased cell proliferation, as reflected by MTT reduction, to 54 ± 8 % ($p<0.01$), 49 ± 8 % ($p<0.001$) and 30 ± 5 % ($p<0.0001$) of control after 24, 48 and 72 h of treatment, respectively (Fig. 1B). Similarly, ATP production was decreased by CTU (10 μM) to 38 ± 3 % ($p<0.001$), 29 ± 4 % ($p<0.001$) and 22 ± 3 % ($p<0.0001$) of control ($p<0.0001$) after 24, 48 and 72 h of treatment, respectively (Fig. 1C).

In these experiments a proportion of cells appeared to remain viable, even after prolonged treatments with higher CTU concentrations. Thus, crystal violet staining showed that some cells remained adherent after 24 and 48 h of CTU treatment (10 μM; Fig. 1D). In further experiments the self-renewal capacity of CTU-treated cells was evaluated directly using the non-adherent, *in vitro* colony-forming mammosphere assay. It was found that treatment of MDA-MB-231 cells with CTU (10 μM, 72 h), followed by a further 72 h recovery period, produced a marked increase in mammosphere formation relative to DMSO control (Fig. 1E). These findings suggest that a cell population with increased self-renewal ability remains after CTU removal.

3.2. CTU treatment enhances the production of pro-inflammatory factors that promote self-renewal of MDA-MB-231 cells

To understand the molecular mechanism of self-renewal we undertook RNA-Seq analysis in MDA-MB-231 cells that had been treated with CTU for 24 h. A total of 16410 genes were identified, of which 131 were up-regulated and 81 were down-regulated (log two-fold cut-off) by CTU (10 μM; 24 h). Bioinformatics analysis with cloud-based IPA software was used to identify biological networks that link differentially expressed genes (Fig. S1). Thus, pro-inflammatory signaling pathways involving IL-6, IL-8, IL-15, IL-17, GM-CSF, STAT3 and NF-κB were all activated in CTU-treated cells (Fig. 2A). Findings from RNA-seq were confirmed using real-time RT-PCR for the quantification of 19 genes (Fig. S2), as summarized in Table S2. A good correlation was noted

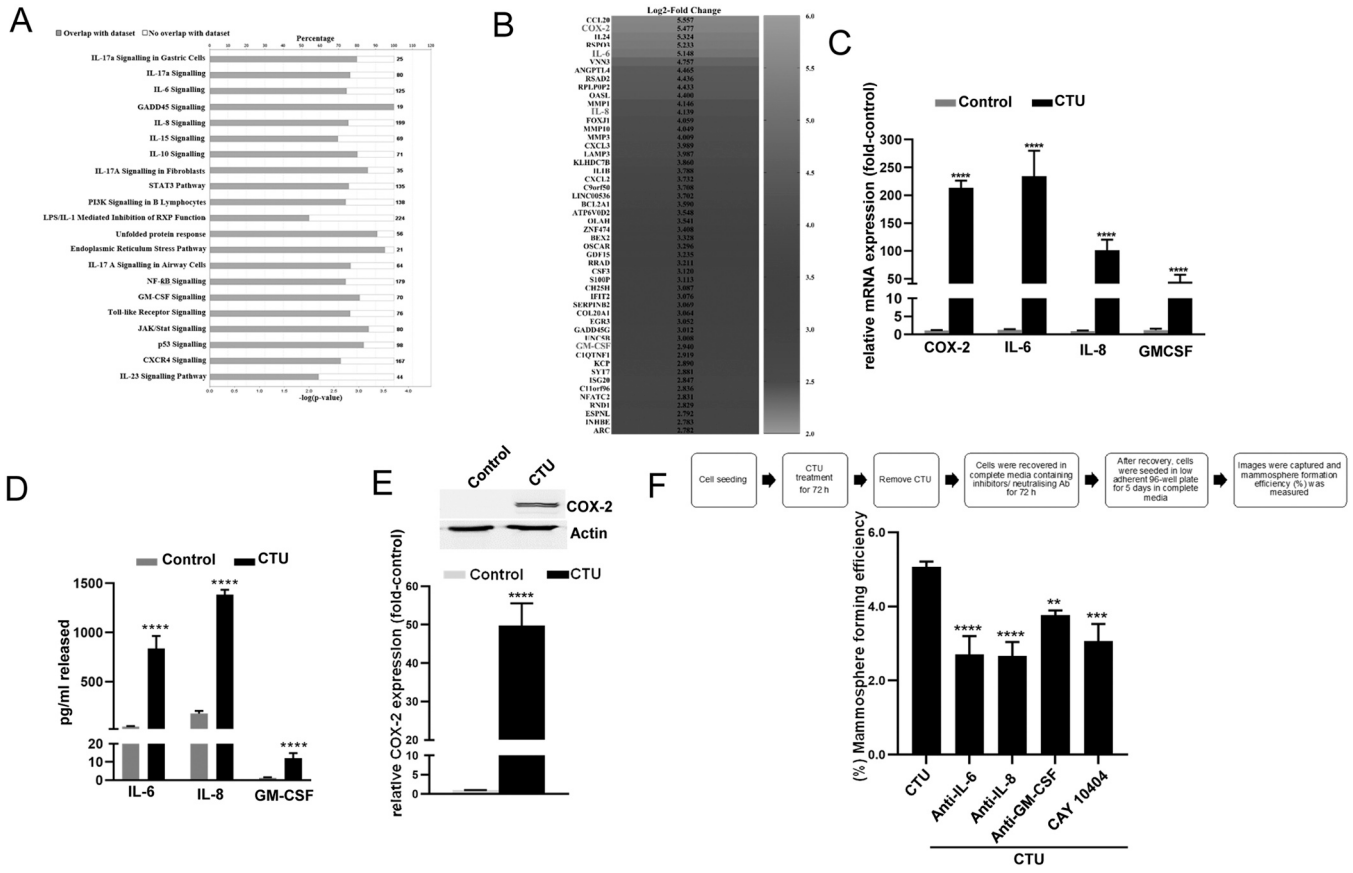

Fig. 2. CTU enhances the production of pro-inflammatory factors that promote self-renewal of MDA-MB-231 cells. (A) RNA-seq analysis indicates increased pro-inflammatory signaling in CTU-treated MDA-MB-231 cells (10 μM, 24 h). The length of the bars indicates the percentage of regulated genes in the pathway; closed bars show genes that overlap with the dataset, and open bars show genes that do not overlap with the dataset. (B) Heat map of the top 50 up-regulated genes from RNA-Seq analysis. Major upregulated genes after CTU treatment are presented in the heat map. Each row represents a single gene, with the expression level shown numerically. (C) Real-time RT-PCR analysis shows increased COX-2, IL-6, IL-8 and GM-CSF mRNA expression in CTU (10 μM, 6 h) treated MDA-MB-231 cells. Cells (1.5×10^5/well) were treated with CTU or DMSO (control). RNA was extracted and quantified. RT-PCR reactions (20 μL) contained SYBR green, reverse transcriptase and appropriate primers. Gene expression was calculated using the ΔΔCT method relative to β-actin. (D) ELISA analysis of cell medium shows increased IL-6, IL-8 and GM-CSF production by CTU (10 μM, 24 h) treated MDA-MB-231 cells. Cells were seeded (1.5×10^5/well) in complete medium, allowed to adhere overnight and serum was removed. Twenty-four h after treatment medium was collected and ELISA assays were performed. (E) Immunoblot analysis shows increased COX-2 protein expression in CTU (10 μM, 24 h)-treated MDA-MB-231 cells. Cells (80–90 % confluence) were harvested and lysed as described in Materials and Methods. Cellular protein was electrophoresed on 7.5–12 % SDS polyacrylamide gels and subjected to Western immunoblotting as described in Materials and Methods. (F) Neutralizing antibodies against pro-inflammatory factors and the COX-2 inhibitor CAY 10404 (0.1 μM) decreased self-renewal ability of CTU-treated MDA-MB-231 cells using the mammosphere assay. Cells (1.5×10^5/well) were incubated overnight, serum was removed and 24 h later cells were treated with CTU (10 μM) for 72 h. Medium was removed and surviving cells were incubated for 72 h in complete medium containing neutralizing antibodies or chemical inhibitors. Cells were seeded (1×10^3/well) on ultra-low attachment surface plates. DMEM/F12 medium containing B27-supplement and EGF (20 ng/ml) was added and incubations were continued for a further 5 d. Images were captured and analyzed as described in Materials and Methods. Data are presented as mean ± standard error (SEM) of three or more independent experiments, with at least two internal replicates. Different from DMSO control: ** $p < 0.01$, *** $p < 0.001$ and **** $p < 0.0001$.

between activation of gene expression by RNA-seq and RT-PCR (r^2=0.9066; Fig. S3). Of the top 50 genes that were upregulated by CTU, 14 were related to inflammation (Fig. 2B). Consistent with previous findings, CTU also activated UPR/ER-stress pathways as indicated by the increases in CHOP and XBP-1s mRNAs (Fig. S4; Choucair et al., 2022).

In view of these findings, four major pro-inflammatory factors (IL-6, IL-8, GM-CSF and COX-2) were selected for further study. Increases in the expression of COX-2, IL-6, IL-8 and GM-CSF mRNAs (Fig. 2C) were corroborated at the protein level using ELISA assays for cytokines (Fig. 2D) and Western blotting for COX-2 (Fig. 2E). The potential role of these pro-inflammatory factors in chemoresistance and anchorage-independent cell growth was assessed. Thus, neutralizing antibodies against IL-6 ($P<0.0001$), IL-8 ($P<0.0001$) and, to a lesser extent GM-CSF ($P<0.01$) suppressed the extent of cell self-renewal in mammosphere formation assays, while the COX-2 inhibitor CAY 10404 (0.1 μM) was similarly active (Fig. 2F). In preliminary studies, a neutralizing antibody against the chemokine CXCL1, which was also increased by CTU treatment (Fig. S2), did not influence mammosphere formation by CTU; a control IgG1 antibody was also inactive (not shown). Together, these results suggest that CTU treatment promotes the self-renewal ability of MDA-MB-231 cells by activating major pro-inflammatory mediators.

3.3. *CTU-mediated inflammatory responses are dependent on NF-κB and XBP1s*

IPA-based network analysis was used to further evaluate CTU-mediated pro-inflammatory signaling and gene activation. Networks were identified in which the transcription factors NF-κB and X box binding protein-1 (spliced form; XBP-1s) were connected to multiple pro-inflammatory factors (Fig. 3A). In further experiments the potential involvement of NF-κB and XBP-1s networks in the regulation of pro-

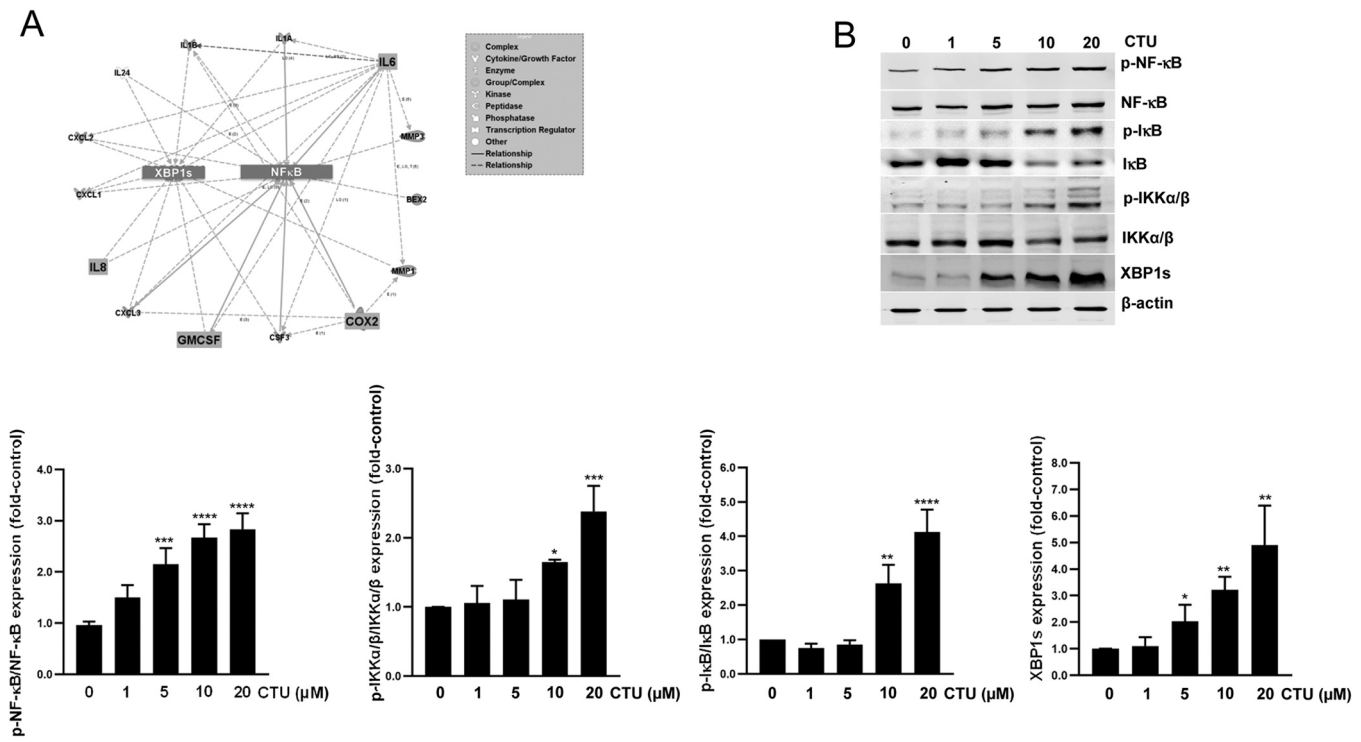

Fig. 3. Activation of NF-κB and XBP1s signalling in CTU-treated MDA-MB-231 cells. (A) Network analysis of the relationships between pro-inflammatory genes and the transcriptional regulators NF-κB and XBP1s. Solid arrows show direct relationships and dotted arrows show indirect relationships between the transcription factors and pro-inflammatory genes. (B) concentration-dependent increases by CTU (0–20 μM, 24 h; with the exception of XBP1s expression at 6 h) in phospho (p)-NF-κB, p-IKK, p-IκB and XBP1s expression in MDA-MB-231 cells. Cells (80–90 % confluence) were harvested and lysed as described in Materials and Methods. Cellular protein was electrophoresed on 7.5–12 % SDS polyacrylamide gels and subjected to Western immunoblotting as described in Materials and Methods. Data are presented as mean ± standard error (SEM) of three or more independent experiments, with at least two internal replicates. Different from DMSO control: * $p < 0.05$, ** $p < 0.01$, *** $p < 0.001$ and **** $p < 0.0001$.

inflammatory mediators was assessed. In initial studies, CTU was found to produce concentration-dependent increases in phospho-NF-κB, IKK, IκB and XBP1s expression in MDA-MB-231 cells (1–20 μM, 24 h; Fig. 3B); these increases were also time-dependent (Figs. S5–S7). In accord with these findings, CTU also activated p-NF-κB and XBP-1s expression in HCC1806 and SKBR3 TNBC cells and cervical carcinoma HeLa cells (Fig. S8).

The role of CTU-mediated NF-κB and XBP1s activation in the formation of pro-inflammatory mediators was tested. Co-treatment of cells with the selective IKK inhibitor BAY 11–7082 (5 μM) attenuated the CTU mediated increase in IL-6, IL-8, GM-CSF and COX-2 expression (Fig. 4A, B), while inhibition of the XBP1s pathway by toyocamycin (0.1 μM) suppressed the CTU-mediated production of IL-6, IL-8 and COX-2, but not GM-CSF (Fig. 4C, D). In confirmation of these findings, knockdown of NF-κB and XBP1s with specific esiRNAs attenuated the CTU-mediated production of the major mediators IL-6 and IL-8 (Fig. 4E, F). These findings indicate that CTU-mediated production of the pro-inflammatory mediators is dependent on NF-κB and XBP1 signaling. The functional significance of NF-κB and XBP1s activation in cell self-renewal was also assessed. Thus, co-treatment of cells with CTU and BAY 11–7082 or toyocamycin effectively decreased mammosphere formation to 52 ± 3 % ($p<0.0001$) and 48 ± 10 % ($p<0.01$) of that by CTU-treated cells, respectively (Fig. 5).

3.4. Inhibition of CTU-mediated IRE1 activation decreases self-renewal of MDA-MB-231 cells and enhances apoptosis

In previous studies CTU was found to activate major ER-stress pathways in MDA-MB-231 cells (Choucair et al., 2022) Apoptotic cell death was dependent on the PERK pathway, but not the IRE1 or ATF6 pathways of ER-stress. Because IRE1 has been reported to activate NF-κB and XBP1 pathways we tested the relationship between CTU treatment and the possible role of IRE1 in the formation of pro-inflammatory mediators (Kaneko et al., 2003). In MDA-MB-231 TNBC cells CTU treatment (6 h) markedly activated IRE1 in concentration-dependent fashion, as shown by the increased p-IRE1/IRE1 ratio (Fig. 6A). Treatment with the IRE1α inhibitor GSK2850163 (10 μM) attenuated the activation of NF-κB and XBP1 splicing in CTU-treated MDA-MB-231 cells (Fig. 6B). Comparative studies were conducted in other cell lines. Thus, CTU (10 μM) also increased p-IRE1 expression in HCC1806 and SKBR3 TNBC cells and the HeLa cervical carcinoma cell line (Fig. S8). Consistent with findings in MDA-MB-231 cells, IRE1 inhibition by GSK2850163 also attenuated CTU-dependent NF-κB and XBP1 activation in HCC1806 cells (10 μM, 6 h; Fig. S9). These findings indicate that CTU activates IRE1/NF-κB/XBP1/inflammatory pathways in several cell types.

The relationship between CTU-mediated IRE1 activation and production of pro-inflammatory factors was assessed using ELISA and immunoblotting assays. Treatment with the IRE1 inhibitor GSK2850163 (10 μM) decreased the production of all four of the pro-inflammatory factors in CTU-treated MDA-MB-231 cells (Fig. 6C, D). Together these findings indicate that CTU-mediated induction of major pro-inflammatory mediators is dependent on the ER-stress sensor IRE1.

Further studies were conducted to assess the functional significance of IRE1 activation in MDA-MB-231 cells. Inhibition of IRE1 by GSK2850163 enhanced apoptotic cell death produced by CTU (10 μM, 24 h; Fig. 6E). GSK2850163 also attenuated the increase in mammosphere formation in CTU-treated cells (Fig. 7). These findings indicate that IRE1 decreases the extent of apoptotic cell death produced by CTU treatment and promotes cell survival. This increases the self-renewal capacity of tumor cells and could lead to the reactivation of tumorigenesis following CTU treatment.

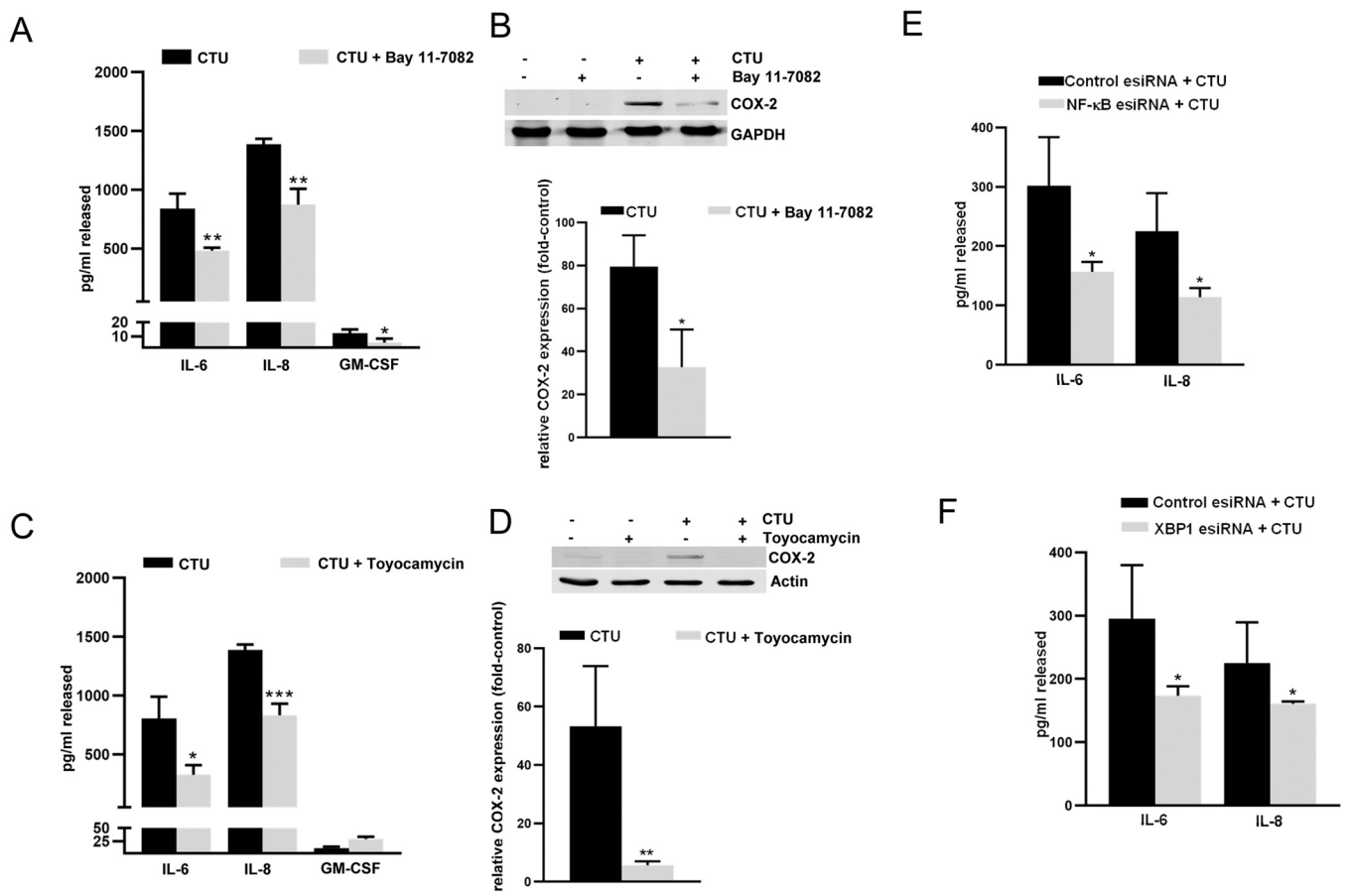

Fig. 4. Inhibition of NF-κB and XBP1s signalling suppresses the production of pro-inflammatory mediators in CTU-treated MDA-MB-231 cells. The IKK inhibitor BAY 11–7082 decreased (A) IL-6, IL-8 and GM-CSF production by ELISA assay and (B) COX-2 expression by immunoblotting. The XBP1s inhibitor toyocamycin attenuated (C) IL-6 and IL-8 production by ELISA assay; and (D) COX-2 expression by immunoblotting analysis. For ELISA analysis cells were seeded (1.5×10^5/well) in complete medium, allowed to adhere overnight and serum was removed. Twenty-four h after treatment medium was collected and ELISA assays were performed. For Western analysis cells (80–90 % confluence) were harvested and lysed as described in Materials and Methods. Cellular protein was electrophoresed on 7.5–12 % SDS polyacrylamide gels and subjected to Western immunoblotting. (E,F) esiRNA-mediated knock-down of (E) NF-κB and (F) XBP1 attenuated IL-6 and IL-8 production by MDA-MB-231 cells. In knock-down studies, cells were seeded (7.5×10^4/well) and incubated overnight in DMEM medium containing 10 % serum. X-tremeGENE siRNA transfection reagent, 2 μg esiRNA and Opti-MEM I were added to cells. 'Scrambled' eGFP esiRNA was used as the negative control. After 48 h, medium was replaced with serum-free Opti-MEM I and 24 h later cells were treated with CTU for 24 h. Data are presented as mean ± standard error (SEM) of three or more independent experiments, with at least two internal replicates. Different from DMSO control: * $p < 0.05$, ** $p < 0.01$ and *** $p < 0.0001$.

4. Discussion

Previous studies have shown that the aryl-ureido fatty acid CTU inhibits mitochondrial complex III and promotes reactive oxygen species production, which activates ER stress and apoptosis in multiple cancer cell lines (Choucair et al., 2022). However, a residual population of MDA-MB-231 cells with an enhanced capacity for self-renewal, as demonstrated by increased mammosphere formation, remained after CTU treatment. In the present study, CTU was found to activate the expression of pro-inflammatory genes that increase cell renewal via NF-κB- and XBP1s-linked pathways that are under the control of the ER-stress sensor IRE1.

Inflammation is tightly linked to the activation of tumorigenesis (Greten and Grivennikov, 2019). Inflammatory mediators, such as cytokines and growth factors, are released by immune cells within the tumor microenvironment and can increase tumor cell proliferation and resistance to cell death, thereby promoting tumor growth and progression. The pro-inflammatory factors COX-2, IL-6, IL-8, and GM-CSF are important features of the tumor microenvironment and promote growth and anchorage-independent colony formation by human TNBC cells (Hartman et al., 2013). GM-CSF reportedly recruits myeloid-derived suppressor cells which regulate T cell immunosuppression and tumor angiogenesis, while IL-8 and IL-6 recruit neutrophils and mesenchymal stem cells (Umansky et al., 2016; Logue et al., 2018). Together, increased COX-2, IL-6 and IL-8 expression is associated with poor prognosis in breast cancer (Hartman et al., 2013; Umansky et al., 2016; Logue et al., 2018; Tawara et al., 2019; Xu et al., 2017).

In the present study the enhanced ability of CTU-treated MDA-MB-231 cells to form mammospheres was attenuated by neutralizing antibodies against IL-6, IL-8 and GM-CSF and by treatment with a COX-2 inhibitor. These findings support a role for pro-inflammatory factors in TNBC self-renewal during recovery from CTU. CTU-mediated production of pro-inflammatory factors was found to be dependent on NF-κB and XBP1 signaling. Thus, NF-κB is an established activator of IL-6, IL-8, GM-CSF and COX-2 gene transcription (Terry et al., 2000; Kunsch et al., 1994; Thomas et al., 1997; Kaltschmidt et al., 2002) while IL-6, IL-8 and COX-2 are also transactivated by XBP1s (Fang et al., 2018; Li et al., 2021; Chopra et al., 2010). Chemical inhibitors of the NF-κB and XBP1 pathways decreased the production of major pro-inflammatory mediators; these findings were confirmed in knockdown studies. Other anticancer agents have also been shown to activate NF-κB in tumor cells. Thus, cisplatin increased the NF-κB-mediated production of IL-1, IL-6, IL-8 and TNF-α in ovarian tumors, which conferred drug resistance (Annunziata et al., 2010; Harrington and Annunziata, 2019). Similarly,

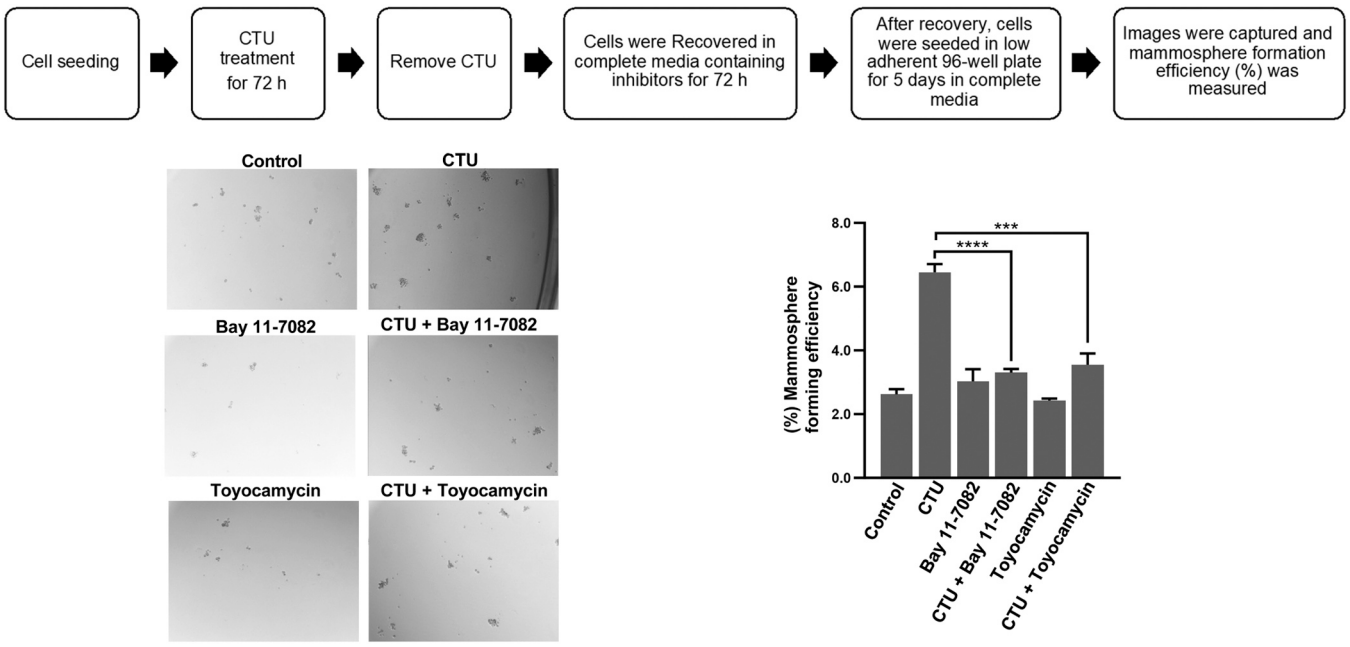

Fig. 5. Effect of NF-κB and XBP1s inhibition on CTU-mediated self-renewal ability in MDA-MB-231 cells. The IKK inhibitor BAY 11–7082 (5 μM) and XBP1s inhibitor toyocamycin (0.1 μM) attenuated self-renewal ability of CTU-treated MDA-MB-231 cells using the mammosphere assay. Cells (1.5×10^5/well) were incubated overnight, serum was removed and 24 h later cells were treated with CTU (10 μM) for 72 h. Medium was removed and surviving cells were incubated for 72 h in complete medium containing chemical inhibitors. Cells were seeded (1×10^3/well) on ultra-low attachment surface plates. DMEM/F12 medium containing B27-supplement and EGF (20 ng/ml) was added and incubations were continued for a further 5 d. Images were captured and analyzed as described in Materials and Methods. Different from CTU alone: *** $p< 0.001$ and **** $p< 0.0001$. Data are presented as mean ± standard error (SEM) of three or more independent experiments, with at least two internal replicates.

treatment of MDA-MB-435 breast cancer cells with paclitaxel activated NF-κB and enhanced expression of the pro-inflammatory COX-2 (Aggarwal et al., 2005).

ER-stress and the UPR are also implicated in the development of drug resistance in breast cancer (Ming et al., 2015). Over 90 % of mammary tumors were positive for XBP1 by immunohistochemistry (Scriven et al., 2009). In the present study, treatment of human MDA-MB-231 breast cancer cells with CTU rapidly increased XBP1s expression. Previous studies have also related ER-stress and UPR activation in TNBC cells to decreased drug sensitivity (Scriven et al., 2009). XBP1s is implicated in relapse of TNBC tumors *in vivo* (Madden et al., 2019) and has been shown to potentiate NF-κB signaling and cellular proliferation (Hu et al., 2015; Barua et al., 2020). Indeed, XBP1s has an important role in the maintenance of cytokine production. Thus, cells transfected with XBP1 siRNA displayed decreased cytokine expression consistent with IRE1–XBP1s signaling (Logue et al., 2018). These findings indicate that XBP1s is an important transcription factor, along with NF-κB, that mediates the production of pro-inflammatory factors by CTU.

CTU-mediated pro-inflammatory cytokine production was regulated by NF-κB and XBP1s and was downstream from the IRE1 pathway of ER-stress. Tumor cells *in vivo* are continuously exposed to ER stress in their microenvironment through hypoxia, low nutrient supply and low pH (Rubio et al., 2011). Moreover, transformed cells have increased demands for protein and lipid for rapid proliferation despite the oxygen- and nutrient-deprived environment (Rubio et al., 2011). To overcome such challenges, cancer cells exploit intrinsic adaptive mechanisms such as the UPR (Rubio et al., 2011). This suggests that the ER stress response may modify the cancer cell microenvironment.

IRE1 is functionally important in maintaining cellular homeostasis by inducing adaptive and prosurvival gene production (Rubio et al., 2011; Urra et al., 2020). It has been reported that breast cancers with a high IRE1 signature were associated with basal-like breast cancers and exhibit increased expression of pro-inflammatory factors (Logue et al., 2018). Inhibiting IRE1 RNase activity reduced the proliferation of breast cancer cells *in vitro* (Logue et al., 2018; Madden et al., 2019). Together, disrupted ER homeostasis that leads to maladaptive UPR signaling is an emerging trait of cancer cells and fosters pro-inflammatory pathways promoting tissue repair and protumorigenic immune responses (Rufo et al., 2022). Indeed, other anti-cancer agents have also been reported to activate IRE1. Thus, paclitaxel activates IRE1 and enhances the production of pro-tumorigenic and pro-inflammatory factors in MDA-MB-231 TNBC cells (Logue et al., 2018). The IRE1-XBP1s pathway is also linked to cell proliferation in other cancers including colon cancer, breast cancer, prostate cancer and melanoma (Madden et al., 2019).

A number of studies have suggested that IRE1 inhibition is potentially valuable as an adjuvant chemotherapy in cancer (Raymundo et al., 2020). IRE1 is an ER-resident type I protein and consists of an N-terminal ER luminal domain, which senses protein-folding status, and a cytosolic C-terminal domain. The latter possesses kinase and endonuclease RNase activities (Lee et al., 2008; Zhou et al., 2006). ER stress activates IRE1 by N-terminal domain homodimerization, autophosphorylation of the kinase domain and a conformational change in the RNase domain. In TNBC, chemical inhibition of the RNase activity of IRE1 prevents the removal of a 26-nucleotide intron to generate the more transcriptionally-active XBP1s (Lee et al., 2008). Inhibition of IRE1 RNase with MKC8866 also decreased pro-inflammatory cytokine production and mammosphere formation in vitro and prevented regrowth of MDA-MB-231 xenografts after paclitaxel withdrawal (Logue et al., 2018). Similarly, inhibition of XBP1 splicing reestablished tamoxifen sensitivity in resistant MCF-7 cells and delayed breast cancer progression in a xenograft model (Ming et al., 2015). In the present study, treatment of cells with the IRE1 inhibitor GSK2850163 attenuated the CTU-dependent increase in IL-6, IL-8 and COX-2 in cell lysates. Under these conditions, mammosphere formation was decreased compared to CTU-alone. GSK2850163 attenuated the phosphorylation of NF-κB and decreased XBP1 splicing by CTU. This indicates that CTU-mediated NF-κB phosphorylation and XBP1 splicing are dependent on IRE1 activation.

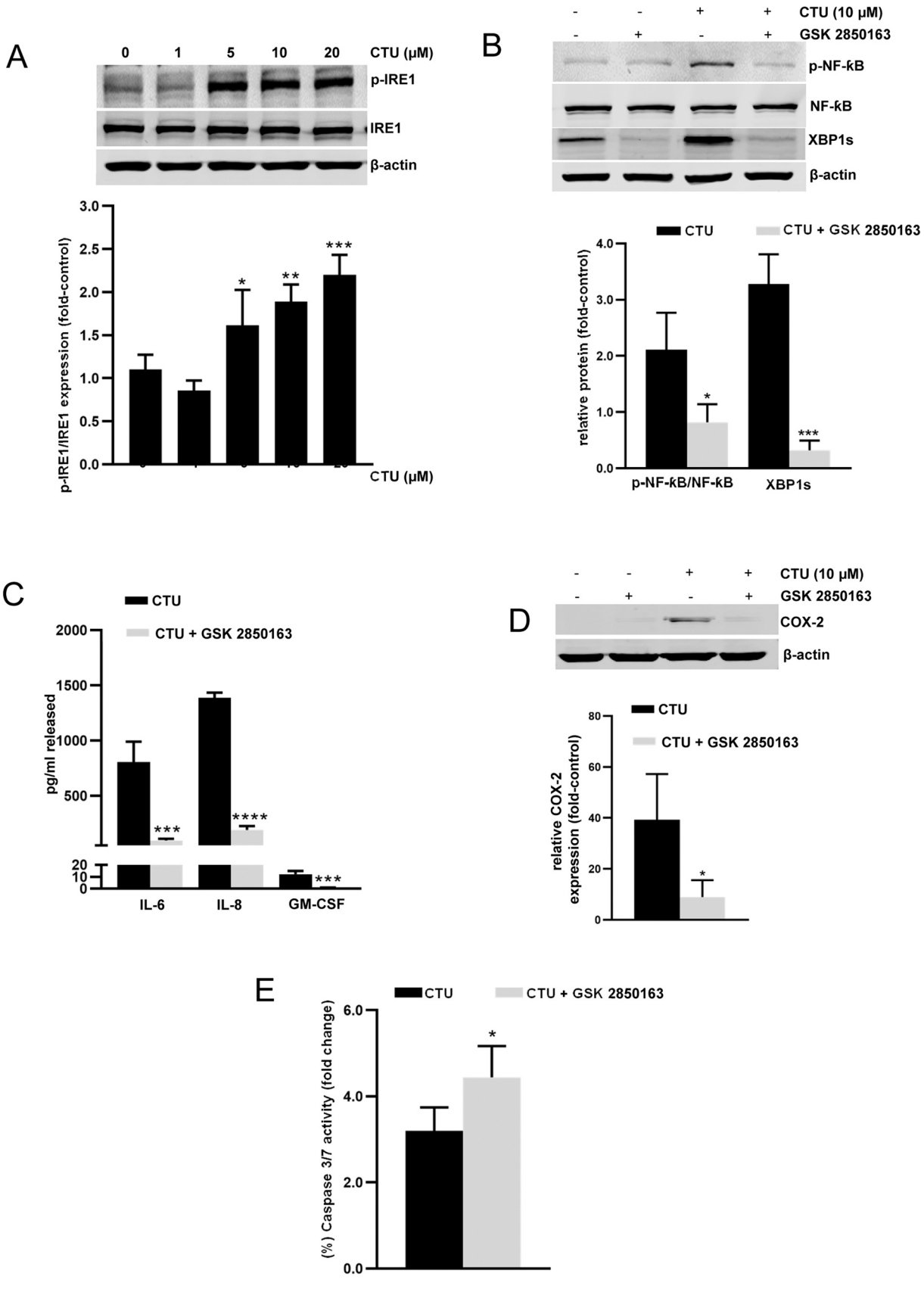

(caption on next page)

Fig. 6. CTU-mediated activation of NF-κB and XBP1 is mediated by the IRE1 pathway of ER stress. (A) Concentration-dependent increases in IRE1 activation in CTU (0–20 μM, 6 h)-treated MDA-MB-231 cells. (B) The CTU-dependent (10 μM) increases in phospho (p)-NF-κB and XBP1s expression (6 h) are attenuated by the IRE1 inhibitor GSK2850163. (C,D) GSK2850163 (10 μM, 24 h) decreased the CTU-mediated formation of (C) pro-inflammatory cytokines and (D) COX-2 expression in MDA-MB-231 cells. (E) Co-treatment with GSK2850163 enhanced CTU-mediated apoptosis (10 μM, 24 h). For ELISA analysis cells were seeded (1.5×10^5/well) in complete medium, allowed to adhere overnight and serum was removed. Twenty-four h after treatment medium was collected and ELISA assays were performed. For Western analysis cells (80–90 % confluence) were harvested and lysed as described in Materials and Methods. Cellular protein was electrophoresed on 7.5–12 % SDS polyacrylamide gels and subjected to Western immunoblotting. In caspase-3/7 assays cells (7×10^3/well) were treated with (10 μM; 24 h) and luminescence was measured as described in Materials and Methods. Data are presented as mean ± standard error (SEM) of three or more independent experiments, with at least two internal replicates. Different from DMSO control: * $p < 0.05$, ** $p < 0.01$, *** $p < 0.001$ and **** $p < 0.0001$.

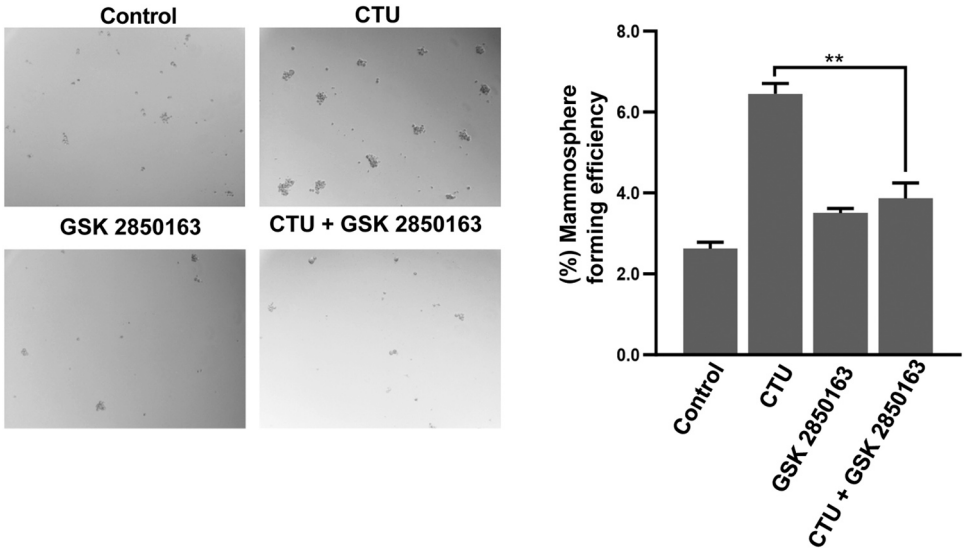

Fig. 7. IRE1 inhibition attenuates self-renewal in CTU-treated MDA-MB-231 cells. The IRE1 inhibitor GSK2850163 (10 μM, 72 h) attenuated the CTU-mediated increase in mammosphere formation. Cells (1.5×10^5/well) were incubated overnight, serum was removed and 24 h later cells were treated with CTU (10 μM) for 72 h. Medium was removed and surviving cells were incubated for 72 h in complete medium containing GSK2850163. Cells were seeded (1×10^3/well) on ultra-low attachment plates. DMEM/F12 medium containing B27-supplement and EGF (20 ng/ml) was added and incubations were continued for a further 5 d. Images were captured and analyzed as described in Materials and Methods. Data are presented as mean ± standard error (SEM) of three or more independent experiments, with at least two internal replicates. Different from CTU alone: ** $p < 0.01$,.

There are no targeted therapies for TNBC, which has a worse prognosis than other breast cancer subtypes. Thus, there is an urgent need for new therapeutic targets and clinical strategies (Logue et al., 2018). CTU is a recently described agent with a novel mode of action. CTU targets the mitochondrion and inhibits complex III of the electron transport chain in tumor cells, which increases the production of reactive oxygen species that activate ER-stress and promote cell killing. However, CTU does not inhibit complex III, promote reactive oxygen species production or activate cell death pathways in well-differentiated cells (Choucair et al., 2022). Further studies are required to explain the selectivity of complex III inhibition in tumor cells by CTU. Such studies may facilitate the identification of novel drug targets and provide useful information on the functional differences between mitochondria in normal and tumor cells. By identifying the specific target for CTU it will be possible to account for the selective killing of tumor cells and undertake modeling approaches to understand the mode of anticancer action of aryl-ureas like CTU in greater detail.

IRE1 RNase inhibitors could enhance the effectiveness of current therapy with existing drugs that activate ER-stress and the production of pro-inflammatory factors (Logue et al., 2018). In the present study, co-treatment of MDA-MB-231 cells with GSK2850163, which is a dual inhibitor of IRE1 kinase and IRE1 RNase activities, decreased NF-κB phosphorylation and XBP1 activation. This enhanced CTU-mediated apoptosis and prevented the activation of pro-tumorigenic factors and self-renewal. Taken together, the present findings suggest that dual inhibition of IRE1 kinase and IRE1 RNase may be a novel approach to optimize the activity of CTU in TNBC.

5. Conclusion

CTU has been shown to selectively inhibit complex III of the mitochondrial electron transport chain in tumor cells, but not in well-differentiated cells, which activates ER-stress and promotes tumor cell death (Choucair et al., 2022). At this time the underlying reasons for the selective inhibition of complex III in tumor cells are unclear. Complex III is a dimer, with each subunit consisting of three catalytic cores and seven supernumerary subunits; complex III activity is increased in breast cancers (Grasso et al., 2020). In future, it may be possible to elucidate structural differences between complex III in tumor and normal cells and this may lead to identification of potential drug target(s) for CTU. At that time, computational investigations, including molecular docking and molecular dynamics simulations could be conducted, which would assist the understanding of the mechanism of tumor selectivity of CTU. The present findings also suggest that, following the activation of ER-stress, CTU upregulates pro-tumorigenic factors in MDA-MB-231 TNBC cells via the IRE1 pathway. This decreases CTU efficacy and promotes the survival of tumor cells. Co-treatment with agents such as the dual inhibitor of IRE1 kinase and IRE1 RNase activities GSK2850163, may be a novel approach that could be used to optimise the clinical efficacy of novel anti-cancer lipids like CTU in TNBC.

Funding

This study was supported by grants from the Australian National Health and Medical Research Council (1031686 and 1145424). The sponsor had no role in study design; in the collection, analysis and

interpretation of data; in the writing of the report; or in the decision to submit the article for publication.

CRediT authorship contribution statement

Michael Murray: Writing – review & editing, Supervision, Project administration, Funding acquisition, Formal analysis, Data curation, Conceptualization. **Tristan Rawling:** Writing – review & editing, Supervision, Project administration, Conceptualization. **Kirsi Bourget:** Writing – review & editing, Investigation. **Hassan Choucair:** Writing – review & editing, Investigation, Conceptualization. **Balasubrahmanyam Umashankar:** Writing – review & editing, Investigation, Conceptualization. **Md Khalilur Rahman:** Writing – review & editing, Writing – original draft, Methodology, Investigation, Formal analysis, Data curation, Conceptualization.

Declaration of Competing Interest

None.

Data Availability

Data will be made available on request.

Appendix A. Supporting information

Supplementary data associated with this article can be found in the online version at doi:10.1016/j.biocel.2024.106571.

References

Aggarwal, B.B., Shishodia, S., Takada, Y., Banerjee, S., Newman, R.A., Bueso-Ramos, C. E., Price, J.E., 2005. Curcumin suppresses the paclitaxel-induced nuclear factor-kappaB pathway in breast cancer cells and inhibits lung metastasis of human breast cancer in nude mice. Clin. Cancer Res. 11, 7490–7498.

Al-Bahlani, S., Al-Lawati, H., Al-Adawi, M., Al-Abri, N., Al-Dhahli, B., Al-Adawi, K., 2017. Fatty acid synthase regulates the chemosensitivity of breast cancer cells to cisplatin-induced apoptosis. Apoptosis 22, 865–876.

Annunziata, C.M., Stavnes, H.T., Kleinberg, L., Berner, A., Hernandez, L.F., Birrer, M.J., Steinberg, S.M., Davidson, B., Kohn, E.C., 2010. Nuclear factor kappaB transcription factors are coexpressed and convey a poor outcome in ovarian cancer. Cancer 116, 3276–3284.

Augimeri, G., Fiorillo, M., Morelli, C., Panza, S., Giordano, C., Barone, I., Catalano, S., Sisci, D., Andò, S., Bonofiglio, D., 2023. The omega-3 docosahexaenoyl ethanolamide reduces CCL5 secretion in triple negative breast cancer cells affecting tumor progression and macrophage recruitment. Cancers 15, 819.

Barua, D., Gupta, A., Gupta, S., 2020. Targeting the IRE1-XBP1 axis to overcome endocrine resistance in breast cancer: opportunities and challenges. Cancer Lett. 486, 29–37.

Bobin-Dubigeon, C., Nazih, H., Croyal, M., Bard, J.-M., 2022. Link between omega 3 fatty acids carried by lipoproteins and breast cancer severity. Nutrients 14, 2461.

Chajès, V., Torres-Mejia, G., Biessy, C., Ortega-Olvera, C., Angeles-Llerenas, A., Ferrari, P., Lazcano-Ponce, E., Romieu, I., 2012. ω-3 and ω-6 Polyunsaturated fatty acid intakes and the risk of breast cancer in Mexican women: impact of obesity status. Cancer Epidemiol. Biomark. Prev. 21, 319–326.

Chopra, S., Giovanelli, P., Alvarado-Vazquez, P.A., Alonso, S., Song, M., Sandoval, T.A., Chae, C.-S., Tan, C., Fonseca, M.M., Gutierrez, S., Jimenez, L., Subbaramaiah, K., Iwawaki, T., Kingsley, P.J., Marnett, L.J., Kossenkov, A.V., Crespo, M.S., Dannenberg, A.J., Glimcher, L.H., Romero-Sandoval, E.A., Cubillos-Ruiz, J.R., 2010. IRE1α-XBP1 signaling in leukocytes controls prostaglandin biosynthesis and pain. Science 365, eaau6499.

Choucair, H., Rahman, M.K., Umashankar, B., Al-Zubaidi, Y., Bourget, K., Chen, Y., Dunstan, C., Rawling, T., Murray, M., 2022. The aryl-ureido fatty acid CTU activates endoplasmic reticulum stress and PERK/NOXA-mediated apoptosis in tumor cells by a dual mitochondrial-targeting mechanism. Cancer Lett. 526, 131–141.

Cui, P.H., Petrovic, N., Murray, M., 2011. The ω-3 epoxide of eicosapentaenoic acid inhibits endothelial cell proliferation by p38 MAP kinase activation and cyclin D1/CDK4 down-regulation. Br. J. Pharmacol. 162, 1143–1155.

Dyari, H.R.E., Rawling, T., Bourget, K., Murray, M., 2014. Synthetic ω-3 epoxyfatty acids as antiproliferative and pro-apoptotic agents in human breast cancer cells. J. Med. Chem. 57, 7459–7464.

Falck, J.R., Kodela, R., Manne, R., Atcha, K.R., Puli, N., Dubasi, N., Manthati, V.L., Capdevila, J.H., Yi, X.-Y., Goldman, D.H., Morisseau, C., Hammock, B.D., Campbell, W.B., 2009. 14,15-Epoxyeicosa-5,8,11-trienoic acid (14,15-EET) surrogates containing epoxide bioisosteres: influence upon vascular relaxation and soluble epoxide hydrolase inhibition. J. Med. Chem. 52, 5069–5075.

Falck, J.R., Koduru, S.R., Mohaptra, S., Manne, R., Atcha, R., Manthati, V.L., Capdevila, J.H., Christian, S., Imig, J.D., Campbell, W.B., 2014. 14,15-Epoxyeicosa-5,8,11-trienoic Acid (14,15-EET) surrogates: carboxylate modifications. J. Med. Chem. 57, 6965–6972.

Fang, P., Luxa Xiang, L., Huang, S., Jin, L., Zhou, G., Zhuge, L., Li, J., Fan, H., Zhou, L., Pan, C., Zheng, Y., 2018. IRE1α-XBP1 signaling pathway regulates IL-6 expression and promotes progression of hepatocellular carcinoma. Oncol. Lett. 16, 4729–4736.

Fleming, I., Rueben, A., Popp, R., Fisslthaler, B., Schrodt, S., Sander, A., Haendeler, J., Falck, J.R., Morisseau, C., Hammock, B.D., Busse, R., 2007. Epoxyeicosatrienoic acids regulate Trp channel dependent Ca^{2+} signaling and hyperpolarization in endothelial cells. Arterioscler. Thromb. Vasc. Biol. 27, 2612–2618.

Grasso, D., Zampieri, L.X., Capelôa, T., Van de Velde, J.A., Sonveaux, P., 2020. Mitochondria in cancer. Cell Stress 4, 114.

Greten, F.R., Grivennikov, S.I., 2019. Inflammation and cancer: triggers, mechanisms, and consequences. Immunity 51, 27–41.

Harrington, B.S., Annunziata, C.M., 2019. NF-κB signaling in ovarian cancer. Cancers 11, 1182.

Hartman, Z.C., Poage, G.M., den Hollander, P., Tsimelzon, A., Hill, J., Panupinthu, N., Zhang, Y., Mazumdar, A., Hilsenbeck, S.G., Mills, G.B., Brown, P.H., 2013. Growth of triple-negative breast cancer cells relies upon coordinate autocrine expression of the proinflammatory cytokines IL-6 and IL-8. Cancer Res. 73, 3470–3480.

Hassan, M., Watari, H., AbuAlmaaty, A., Ohba, Y., Sakuragi, N., 2014. Apoptosis and molecular targeting therapy in cancer. Biomed. Res. Int. 2014, 150845.

Hetz, C., Zhang, K., Kaufman, R.J., 2020. Mechanisms, regulation and functions of the unfolded protein response. Nat. Rev. Mol. Cell. Biol. 21, 421–438.

Hu, R., Warri, A., Jin, L., Zwart, A., Riggins, R.B., Fang, H.B., Clarke, R., 2015. NF-kappaB signaling is required for XBP1 (unspliced and spliced)-mediated effects on antiestrogen responsiveness and cell fate decisions in breast cancer. Mol. Cell Biol. 35, 379–390.

Inceoglu, B., Jinks, S.L., Ulu, A., Hegedus, C.M., Georgi, K., Schmelzer, K.R., Wagner, K., Jones, P.D., Morisseau, C., Hammock, B.D., 2008. Soluble epoxide hydrolase and epoxyeicosatrienoic acids modulate two distinct analgesic pathways. Proc. Natl. Acad. Sci. 105, 18901–18906.

Kaltschmidt, B., Linker, R.A., Deng, J., Kaltschmidt, C., 2002. Cyclooxygenase-2 is a neuronal target gene of NF-kappaB. BMC Mol. Biol. 3, 16.

Kaneko, M., Niinuma, Y., Nomura, Y., 2003. Activation signal of nuclear factor-κB in response to endoplasmic reticulum stress is transduced via IRE1 and tumor necrosis factor receptor-associated factor 2. Biol. Pharm. Bull. 26, 931–935.

Kimata, Y., Ishiwata-Kimata, Y., Ito, T., Hirata, A., Suzuki, T., Oikawa, D., Takeuchi, M., Kohno, K., 2007. Two regulatory steps of ER-stress sensor IRE1 involving its cluster formation and interaction with unfolded proteins. J. Cell Biol. 179, 75–86.

Kunsch, C., Lang, R.K., Rosen, C.A., Shannon, M.F., 1994. Synergistic transcriptional activation of the IL-8 gene by NF-kappaB p65 (RelA) and NF-IL-6. J. Immunol. 153, 153–164.

Lee, K.P., Dey, M., Neculai, D., Cao, C., Dever, T.E., Sicheri, F., 2008. Structure of the dual enzyme IRE1 reveals the basis for catalysis and regulation in nonconventional RNA splicing. Cell 132, 89–100.

Li, M., Xie, Y., Zhao, K., Chen, K., Cao, Y., Zhang, J., Han, M., Hu, L., He, R., Wang, D., Li, H., 2021. Endoplasmic reticulum stress exacerbates inflammation in chronic rhinosinusitis with nasal polyps via the transcription factor XBP1. Clin. Immunol. 223, 108659.

Liu, Y., Wang, R., Li, J., Rao, J., Li, W., Falck, J.R., Manthati, V.L., Medhora, M., Jacobs, E.R., Zhu, D., 2001. Stable EET urea agonist and soluble epoxide hydrolase inhibitor regulate rat pulmonary arteries through TRPCs. Hypertens. Res. 34, 630–639.

Logue, S.E., McGrath, E.P., Cleary, P., Greene, S., Mnich, K., Almanza, A., Chevet, E., Dwyer, R.M., Oommen, A., Legembre, P., Godey, F., Madden, E.C., Leuzzi, B., Obacz, J., Zeng, Q., Patterson, J.B., Jager, R., Gorman, A.M., Samali, A., 2018. Inhibition of IRE1 RNase activity modulates the tumor cell secretome and enhances response to chemotherapy. Nat. Commun. 9, 3267.

Luo, D., Fan, N., Zhang, X., Ngo, F.Y., Zhao, J., Zhao, W., Huang, M., Li, D., Wang, Y., Rong, J., 2022. Covalent inhibition of endoplasmic reticulum chaperone GRP78 disconnects the transduction of ER stress signals to inflammation and lipid accumulation in diet-induced obese mice. eLife 11, e72182.

Madden, E., Logue, S.E., Healy, S.J., Manie, S., Samali, A., 2019. The role of the unfolded protein response in cancer progression: from oncogenesis to chemoresistance. Biol. Cell. 111, 1–17.

Ming, J., Ruan, S., Wang, M., Ye, D., Fan, N., Meng, Q., Tian, B., Huang, T., 2015. A novel chemical, STF-083010, reverses tamoxifen-related drug resistance in breast cancer by inhibiting IRE1/XBP1. Oncotarget 6, 40692–40703.

Murray, M., 1992. Participation of a cytochrome P450 enzyme from the 2C subfamily in progesterone 21-hydroxylation in sheep liver. J. Steroid Biochem. 43, 591–593.

Newell, M., Goruk, S., Mazurak, V., Postovit, L., Field, C.J., 2019. Role of docosahexaenoic acid in enhancement of docetaxel action in patient-derived breast cancer xenografts. Breast Cancer Res. Treat. 177, 357–367.

Rawling, T., Choucair, H., Koolaji, N., Bourget, K., Allison, S.E., Chen, Y.J., Dunstan, C. R., Murray, M., 2017. A novel arylurea fatty acid that targets the mitochondrion and depletes cardiolipin to promote killing of breast cancer cells. J. Med. Chem. 60, 8661–8666.

Raymundo, D.P., Doultsinos, D., Guillory, X., Carlesso, A., Eriksson, L.A., Chevet, E., 2020. Pharmacological targeting of IRE1 in cancer. Trends Cancer 6, 1018–1030.

Rendic, S., Guengerich, F.P., 2015. Survey of human oxidoreductases and cytochrome P450 enzymes involved in the metabolism of xenobiotic and natural chemicals. Chem. Res. Toxicol. 28, 38–42.

Rose, D.P., Connolly, J.M., 2000. Regulation of tumor angiogenesis by dietary fatty acids and eicosanoids. Nutr. Cancer 37, 119–127.

Rubio, C., Pincus, D., Korennykh, A., Schuck, S., El-Samad, H., Walter, P., 2011. Homeostatic adaptation to endoplasmic reticulum stress depends on IRE1 kinase activity. J. Cell Biol. 193, 171–184.
Rufo, N., Yang, Y., De Vleeschouwer, S., Agostinis, P., 2022. The "Yin and Yang" of unfolded protein response in cancer and immunogenic cell death. Cells 11, 2899.
Scriven, P., Coulson, S., Haines, R., Balasubramanian, S., Cross, S., Wyld, L., 2009. Activation and clinical significance of the unfolded protein response in breast cancer. Br. J. Cancer 101, 1692–1698.
Spector, A.A., 2009. Arachidonic acid cytochrome P450 epoxygenase pathway. J. Lipid Res. 50, S52–56.
Tawara, K., Scott, H., Emathinger, J., Wolf, C., LaJoie, D., Hedeen, D., Bond, L., Montgomery, P., Jorcyk, C., 2019. HIGH expression of OSM and IL-6 are associated with decreased breast cancer survival: synergistic induction of IL-6 secretion by OSM and IL-1β. Oncotarget 10, 2068–2085.
Terry, C.F., Loukaci, V., Green, F.R., 2000. Cooperative influence of genetic polymorphisms on interleukin 6 transcriptional regulation. J. Biol. Chem. 275, 18138–18144.
Thomas, R.S., Tymms, M.J., McKinlay, L.H., Shannon, M.F., Seth, A., Kola, I., 1997. ETS1, NFkappaB and AP1 synergistically transactivate the human GM-CSF promoter. Oncogene 14, 2845–2855.
Umansky, V., Blattner, C., Gebhardt, C., Utikal, J., 2016. The role of myeloid-derived suppressor cells (MDSC) in cancer progression. Vaccines 4, 36.
Urra, H., Pihán, P., Hetz, C., 2020. The UPRosome–decoding novel biological outputs of IRE1α function. J. Cell. Sci. 133, jcs218107.
Wiseman, R.L., Mesgarzadeh, J.S., Hendershot, L.M., 2022. Reshaping endoplasmic reticulum quality control through the unfolded protein response. Mol. Cell. 82, 1477–1491.
Woodcock, C.C., Huang, Y., Woodcock, S.R., Salvatore, S.R., Singh, B., Golin-Bisello, F., Davidson, N.E., Neumann, C.A., Freeman, B.A., Wendell, S.G., 2018. Nitro-fatty acid inhibition of triple-negative breast cancer cell viability, migration, invasion, and tumor growth. J. Biol. Chem. 293, 1120–1137.
Xu, C., Bailly-Maitre, B., Reed, J.C., 2005. Endoplasmic reticulum stress: cell life and death decisions. J. Clin. Invest. 115, 2656–2664.
Xu, F., Li, M., Zhang, C., Cui, J., Liu, J., Li, J., Jiang, H., 2017. Clinicopathological and prognostic significance of COX-2 immunohistochemical expression in breast cancer: a meta-analysis. Oncotarget 8, 6003–6012.
Zhang, G., Panigrahy, D., Mahakian, L.M., Yang, J., Liu, J.Y., Stephen Lee, K.S., Wettersten, H.I., Ulu, A., Hu, X., Tam, S., Hwang, S.H., Ingham, E.S., Kieran, M.W., Weiss, R.H., Ferrara, K.W., Hammock, B.D., 2013. Epoxy metabolites of docosahexaenoic acid (DHA) inhibit angiogenesis, tumor growth, and metastasis. Proc. Natl. Acad. Sci. 110, 6530–6535.
Zhou, J., Liu, C.Y., Back, S.H., Clark, R.L., Peisach, D., Xu, Z., Kaufman, R.J., 2006. The crystal structure of human IRE1 luminal domain reveals a conserved dimerization interface required for activation of the unfolded protein response. Proc. Natl. Acad. Sci 103, 14343–14348.